TURUN
YLIOPISTO
UNIVERSITY
OF TURKU

GEOCHEMISTRY OF FELSIC, MAFIC AND ULTRAMAFIC ROCKS IN THE SUPRASUBDUCTION ZONE MAWAT OPHIOLITE, NORTHEAST IRAQ

Heider Al Humadi

TURUN YLIOPISTON JULKAISUJA – ANNALES UNIVERSITATIS TURKUENSIS
SARJA – SER. AII OSA – TOM. 385 | BIOLOGICA – GEOGRAPHICA – GEOLOGICA | TURKU 2021

TURUN
YLIOPISTO
UNIVERSITY
OF TURKU

GEOCHEMISTRY OF FELSIC, MAFIC AND ULTRAMAFIC ROCKS IN THE SUPRASUBDUCTION ZONE MAWAT OPHIOLITE, NORTHEAST IRAQ

Heider Al Humadi

TURUN YLIOPISTON JULKAISUJA – ANNALES UNIVERSITATIS TURKUENSIS
SARJA – SER. AII OSA – TOM. 385 | BIOLOGICA – GEOGRAPHICA – GEOLOGICA | TURKU 2021

University of Turku

Faculty of Science
Department of Geography and Geology
Geology and Mineralogy
Doctoral programme in Biology, Geography and Geology (BGG)

Supervised by

Adjunct Professor, University Lecturer,
Markku Väisänen
University of Turku
Finland

Professor, Sabah A. Ismail
University of Kirkuk
Iraq

Reviewed by

Adjunct Professor, Senior Researcher,
Tapio Halkoaho
Geological Survey of Finlnad
Finland

Associated Professor, Kristoffer Szilas
University of Copenhagen
Denmark

Opponent

Adjunct Professor, Academy Research Fellow,
Jussi S. Heinonen
University of Helsinki
Finland

ISBN 978-951-29-8658-3 (PRINT)
ISBN 978-951-29-8659-0 (PDF)
ISSN 0082-6979 (Print)
ISSN 2343-3183 (Online)
Painosalama, Turku, Finland 2021

UNIVERSITY OF TURKU
Faculty of Science
Department of Geography and Geology
Geology and Mineralogy
HEIDER AL HUMADI: Geochemistry of Felsic, Mafic and Ultramafic Rocks in the Suprasubduction Zone Mawat Ophiolite, Northeast Iraq
Doctoral Dissertation, 111 pp.
Doctoral Programme in Biology, Geography and Geology (BGG)
October 2021

ABSTRACT

The Mawat ophiolite is a remnant from the Neotethyan oceanic lithosphere exposed within the Zagros Suture Zone, northeastern Iraq. This thesis focuses on the evolution of the mantle-derived magma and their temporally and spatially associated evolution during the late Cretaceous-Eocene. The isotope geology in Mawat is based on zircon and monazite U-Pb dating, and zircon Hf isotopes from felsic dykes and a gabbro. The zircon results give ages between 222 and 38 Ma interpreted to be related to radiogenic Pb mobility and Pb loss. The monazite 94.6 ± 1.2 Ma age is considered as a crystallization age of the felsic dykes and the oldest zircons in gabbro provide the age of 81.2 ± 2.5 Ma which is the crystallisation age of the gabbro. The gabbro is interpreted to be related to later rifting above the suprasubduction zone. The youngest ages ~ 40 Ma are raleted to crustal extension. The negative zircon initial ε_{Hf} values for the felsic dykes indicate that the magma comes from an older source. The positive zircon initial ε_{Hf} values for gabbro suggest that the magma comes from a juvenile source.

The felsic dykes occur in two types: tonalites and granites. The dykes also occur in the western part as a plagiogranite and the central part as a leucogranite. Both types are mixed in various proportions in the east. The eastern tonalities are weakly peraluminous to metaluminous and are low in K_2O, TiO_2, and high in Na_2O. They have low MgO, Cr, and Ni contents and low Sr/Y compared to the western ones where these are high and similar to adakites. These were derived by partial melting of the subducted oceanic slab. The eastern tonalities underwent hornblende and plagioclase fractionation in a shallow-level magma chamber modifying their original compositions. The eastern granites are strongly peraluminous, moderate to high in K_2O, Pb and Na_2O, and very low in TiO_2. Their melts are derived from psammitic sediments on the top of the subducted slab. Parental melts of the tonalities and granites partially mixed in shallow magma chambers.

The basalts and ultramafic rocks are extremely depleted in the LILE and some HFSE elements. They plot below the N-MORB reference line suggesting that these elements have been mobile. The basaltic and ultramafic rocks resemble the arc boninites related to subduction initiation setting. This is confirmed with Ti/1000 vs. V diagram. This suggests that these rocks formed in the same forearc region. The undepleted pattern of the gabbros plot parallel to the N-MORB reference line and within the MORB field in the V vs. Ti/1000 diagram. This is an indication of rifting in an extensional setting above the subduction zone. The geochemical data is consistent with the tectonic setting for suprasubduction zone ophiolite.

KEYWORDS: felsic dyke, U-Pb geochronology, mafic, Mawat ophiolite, Neotethyan ocean, Zagros, Iraq

TURUN YLIOPISTO
Matemaattis-luonnontieteellinen tiedekunta
Maantieteen ja geologian laitos
Geologia ja Mineralogia
HEIDER AL HUMADI: Koillis-Irakissa suprasubduktiovyöhykkeellä muodostuneen Mawatin ofioliitin felsisten, mafisten ja ultramafisten kivien geokemia
Väitöskirja, 111 sivua
Biologian, maantieteen ja geologian tohtoriohjelma
Lokakuu 2021

TIIVISTELMÄ

Mawatin ofioliitti on jäänne muinaisesta Neotethyanin merellisestä kuoresta Zagrosin sutuurivyöhykkeellä Koillis-Irakissa. Tässä väitöskirjassa keskitytään Mawatin vaippaperäisten magmojen evoluutioon sekä niiden ajallisiin ja alueellisiin muutoksiin Ylä-Liitu-Eoseenin ajanjaksolla. Mawatin isotooppigeologia perustuu U-Pb zirkoni- ja monatsiitti-ikämäärityksiin sekä zirkonin Hf isotooppeihin felsisistä juonista ja gabrosta. Zirkonit antavat iät 222–38 Ma, joiden on tulkittu liittyvän radiogeenisen lyijyn mobiilisuuteen zirkonissa ja lyijyn karkaamiseen zirkonista. Monatsiitista saatua 94.6 ± 1.2 Ma ikää pidetään felsisen juonen kiteytymisikänä. Gabron vanhimmat zirkonit antavat iän 81.2 ± 2.5 Ma, joka on gabron kiteytymisikä. Gabbron tulkitaan liittyvän ekstensioon subduktiovyöhykkeen yläpuolelle. Nuorimmat ~40 Ma iät liittyvät kuoren myöhempään ekstensioon. Felsisten juonien zirkonien negatiiviset ε_{Hf} arvot osoittavat, että magma tulee vanhemmasta lähteestä ja gabron zirkonien positiiviset ε_{Hf} arvot viittaavat juveniiliin lähteeseen.

Felsisiä juonia esiintyy kahta tyyppä: tonaliitteja ja graniitteja. Juonet esiintyvät myös Mawatin länsiosassa plagiograniittina ja keskiosassa leukograniittina. Molemmat tyypit ovat sekoittuneet itäosissa eri suhteissa. Itäisten tonaliitien koostumukset ovat heikosti peralumiinisista metaluminisiin ja niillä on alhaiset K_2O ja TiO_2 ja korkeat Na_2O pitoisuudet. MgO, Cr ja Ni pitoisuudet ja Sr/Y suhde ovat alhaisempia kuin läntisissä juonissa, joissa nämä ovat hyvin korkeita ja muistuttavat adakiitteja, jotka ovat peräisin subduktoituneen merellisen laatan osittaisesta sulamisesta. Itäisten tonaliittien sarvivälke ja plagioklaasi fraktioituvat matalalla sijaitsevassa magmasäiliössä, ja se muokkasi magman alkuperäistä koostumusta. Itäiset graniitit ovat voimakkaasti peraluminaalisia ja niillä on korkeat K_2O, Pb ja Na_2O ja hyvin alhaiset TiO_2 pitoisuudet. Ne ovat peräisin subduktoituneen merellisen laatan päällä olevista psammittista sedimenteistä. Tonaliittien ja graniittien alkusulat ovat osittain sekoittuneet matalalla sijainneessa magmasäiliössä.

Basaltit ja ultramafiset kivet ovat erittäin köyhtyneitä LILE- ja HFSE-alkuaineista. Ne ovat N-MORBiin verrattuna köyhtyneitä, mikä viittaa näiden alkuaineiden mobiilisuuteen. Basalttiset ja ultramafiset kivet muistuttavat subduktion alkuvaiheessa syntyneitä kaarityypin boniniitteja. Sitä esitetään Ti/1000 vs. V-diagrammilla. Tämä viittaa siihen, että nämä muodostuivat samassa kaaren etualtaassa. Gabrojen yhtenäiset geokemialliset koostumukset muistuttavat N-MORB:ia ja osuvat V vs. Ti/1000 -diagrammissa MORB-kenttään. Tämä viittaa riftiytymiseen subduktiovyöhykkeen yläpuolella. Geokemiallinen aineisto on kokonaisuudessaan samanlaista kuin suprasubduktiovyöhykkeen ofioliiteilla.

AVAINSANAT: Felsinen juoni, U-Pb geokronologia, mafinen, Mawatin ofioliitti, Neotethyanin meri, Zagros, Irak

جامعة توركو
كلية العلوم
قسم الجيوغرافيا والجيولوجيا
الجيولوجيا والمعادن
حيدر صبري الحمادي: جيوكيميائية الصخورالفلسية والمافية وفوق المافية في ماوات أفيوليت المتكون في نطاق ما فوق الأندساس (الغوران), شمال شرق العراق.
أطروحة , 111 صفحة
برنامج الدكتوراه في البيولوجيا والجيوغرافيا والجيولوجيا (ب ج ج)
تشرين أول 2021

الملخص

ماوات أوفيولايت تمثل بقايا من الوشاح الاعلى للقشرة المحيطية النيوتيثسية المنكشفة ضمن منطقة التحام زاغروس ، شمال شرق العراق. تركزهذه الأطروحة على تطورالماكما المشتقة من الجبة والتطورات الزمانية والمكانية المصاحبة لها خلال أواخرالعصر الطباشيري - الإيوسيني. أستندت دراسة جيولوجيا النظائر في ماوات افيولايت على معدني الزركون والمونازايت من خلال احتساب الاعمار بواسطة اليورانيوم - رصاص , ونظائر الهافنيوم في معدن الزركون للصخور الفلسية و لصخرة الكابرو. تظهر النتائج ان معدن الزركون يعطي أعمارا بين 222 و 38 مليون سنة, وهذه فسرت بانها مرتبطة بحركية الرصاص المشع وفقدان الرصاص. أعتبرعمرالمونازيت 1.2 ± 94.6 مليون سنة بمثابة عمر تبلور السدود الفلزية. أقدم حبيبات معدن الزركون في صخرة الكابرو تعطي عمر 2.5 ± 81.2 مليون سنة وهو يمثل عمرتبلور معدن الزركون في صخرة الكابرو. وتواجد الكابرو قد فسر بأنه مرتبط بالصدع المتكون لاحقا فوق منطقة الأندساس. أما الاعمارالحديثة المقاربة ل 40 مليون سنة فهي مرتبطة بتمدد القشرة. وتشير قيم εHf الاولية السالبة في الزركون الى ان صهارة السدود الفلسية جاءت من مصدر اقدم, بينما قيم εHf الأولية الموجبة في معدن الزكون لصخرة الكابرو تشير الى ان صهير الكابرو جاء من مصدر حديث عمريا.

الصخور الفلسية (السدود) توجدعلى نوعين: النوع الاول هوالتونلايت والثاني الكرانايت. وتتواجد هذه الصخور في الجزء الغربي من ماوات افيولايت على شكل بلاجيوكرانيت وأيضًا في الجزء المركزي من الافيولايت على شكل ليوكوكرانيت. كلا هذين النوعين قد أختلطا معا بنسب مختلفة وأنكشفا في الجزء الشرقي من الافيولايت. تتميز صخور التونلايت الواقعة في الجزء الشرقي لماوات افيولايت بارتفاع ضعيف نسبيا بقيمة أوكسيد الالمنيوم مقابل قيم أوكسيد الصوديوم والبوتاسيوم والكالسيوم (برالومينياس) الى أرتفاعا اكثر نسبيا (متالومينياس). تتميزهذه الصخوربأحتوائها على القليل من اكاسيد البوتاسيوم والتيتانيوم وقيم مرتفعة من محتوى اوكسيد الصوديوم , كما تحتوي على القليل من اوكسيد المغنيسوم والكروم والنيكل, اضافة الى احتوائها على نسب منخفضة من(ألسترونتيوم/ أتريوم) مقارنة بتلك النسب الموجودة في صخورالجزء الغربي من الافيولايت والتي تشابة صخورالأدكايت.هذه الصخوراشتقت نتيجة عملية الذوبان الجزئي للصفيحة (البلاطة) المحيطية المندسة. خضعت معادن الهورنبلند والبلاجوكليس في صخور التونلايت في الجزء الشرقي من الافيولايت الى تبلورتجزيئي في حجرة الصهيرذات العمق الضحل لتغيربذلك مكوناتها الاصلية. صخورالكرانيت شرقي ماوات افيولايت تتميزبارتفاع محتوى اوكسيد الالمنيوم مقابل اوكسيد الصديوم والبوتاسيوم اي انها (برالومينياس) كما انها معتدل الى عالية المحتوى لأوكسيد البوتاسيوم وعنصرالرصاص بينما محتوى أوكسيد التيتانيوم منخفظ جدا. صهيرهذه الصخورمشتق من الرسوبيات الرملية المتواجدة على السطح العلوي للصفيحة المندسة. الصهيرالأم لصخورالتونلايت والكرانيت قد امتزج جزئيا في حجرات الصهير ذات العمق الضحل.

البازلت والصخورالفوق قاعدية تكون مستنفذة بشكل كبيرلعناصرالليثوفيلي ذات نصف القطرالعالي LILE وبعض العناصر ذات مجال الجهد العالي HFSE.هذه الصخورتقع في المخطط أسفل خط المرجع N-MORB مما تقترح بان هذه العناصر كانت متحركة. الصخورالبازلتية والفوق مافية تشابه القوس البونينايتي المتكون نتيجة أرتباطه بأول تشكل في بداية الاندساس, وهذا يقترح بان هذه الصخور قد تكونت في نفس نطاق بيئة مقدمة الجزر القوسية , وهذا ما يوكده مخطط العلاقة بين عنصري الفناديوم مع التيتانيوم. الكابرو يظهر نمط غير مستنفذ ويقع في موازاة خط مخخط العلاقة N-MORB وضمن حقل MORB في بين عنصري الفناديوم والتيتانيوم. وهذا يشيرالى التصدع في وضعية التمدد فوق منطقة الاندساس. تتوافق البيانات الجيوكيميائية مع التشكل التكتوني لنطاق الافيولات في نطاق فوق الاندساس (الغوران).

الكلمات الدالة: الصخرالفلسي, اليورانيوم - رصاص جيوكرونولوجي, الصخورالمافية, ماوات افيولايت, بحر النيو تثيس, زاغروس , العراق

Table of Contents

Abbreviations

AHOB	Alpine-Himalayan Orogenic Belt
BSE	Back-scattered electron
E-MORB	Enriched mid-ocean ridge basalt
HFSE	High field strength element
HREE	Heavy rare earth element
ICP-MS	Inductively coupled plasma mass spectrometer
IZSZ	Iraqi Zagros Suture Zone
LILE	Large ion lithophile element
LREE	Light rare earth element
Ma	Mega annum, millions of years
MO	Mawat Ophiolite
MORB	Mid-ocean ridge basalt
MREE	Middle rare earth element
N-MORB	Normal Mid-ocean ridge basalt
OIB	Ocean island basalt
PM	Primitive mantle
REE	Rare earth element
SEM	Scanning electron microscope
TAS	Total alkali vs. silica
XRF	X-Ray Fluorescence Spectrometry
ZOB	Zagros Orogenic Belt

List of Original Publications

This dissertation is based on the following original publications, which are referred to the text by their Roman numerals:

I. Al Humadi, H., Väisänen, M., Ismail, S. A., Kara, J., O'Brien, H., Lahaye, Y., & Lehtonen, M. (2019). U–Pb geochronology and Hf isotope data from the Late Cretaceous Mawat ophiolite, NE Iraq. *Heliyon*, 5; e02721 https://doi.org/10.1016/j.heliyon.2019.e02721

II. Al Humadi, H., Väisänen, M., Ismail, S. A., Lehtonen, M. & Johanson, B. (2021). Subducted basalts and sediments as sources for felsic dykes in the Mawat ophiolite, NE Iraq. *Ofioliti*, 46(1), 27–41. https://doi.org/10.4454/ofioliti.v46i1.536

III. Al Humadi, H., Väisänen, M. & Ismail, S. A. Geochemical characteristics of mafic and ultramafic rocks of the suprasubduction zone Mawat ophiolite, NE Iraq. *Manuscript.*

1 Introduction

1.1 Ophiolite

An ophiolite is an association of ultramafic to felsic rock assemblages formed in a variety of plate tectonic settings, including mid-oceanic ridges, extensional fore-arcs, extensional arcs, back-arc basins and rifted continental margins (e.g., Moores, 1982; Lippard et al., 1986; Parson et al., 1992; Dilek and Robinson et al., 2003; Kusky 2004, Kusky et al., 2011). The ophiolites record the tectonic and magmatic events that occurred in ancient oceanic basins and adjacent continental margins, from rift to rift-drift, oceanic spreading, subduction and accretion (Dilek and Furnes, 2011). An ophiolite may be obducted onto continental margins or incorporated into accretionary prisms and orogens (Dilek and Furnes, 2009).

Ophiolites are classified into two main types: subduction-related and subduction-unrelated types (Dilek and Furnes, 2014; Furnes and Dilek, 2017; Furnes et al, 2020). The subduction-related types, i.e., suprasubduction zone ophiolites, form as part of the upper plate of a subduction zone. They are subdivided into backarc, forearc, backarc-forearc and volcanic arc ophiolites. In the the subduction-unrelated ophiolites their magmatic signatures are not affected by subduction processes. They are subdivided into rift, continental margin, mid-ocean ridge and plume-type ophiolites (Dilek and Furnes, 2011, 2014). A complete ophiolite sequence grades upward from bottom to top and consists of upper mantle peridotite, layered ultramafic-mafic rocks, layered to isotropic gabbros, sheeted dykes, extrusive rocks (lavas) and a sedimentary cover (Anonymous, 1972). The ophiolites record significant evidences for tectonic and magmatic processes from rift-drift through accretionary and collisional stages of continental margin evolution in various tectonic settings (Dilek and Robinson, 2003).

Ophiolites are reported from various parts of the world with ages from Archean to Cenozoic (Furnes and Dilek, 2017). There are Archean ophiolites, e.g., along the margin of microcontinent in the North China Craton (Santosh et al., 2016) and the Proterozoic 870-627 Ma ophiolite suite occur, e.g., in Fennoscandian Shield (Kontinen, 1987) and Arabian Shield (Dilek and Ahmed, 2003). The Cenozoic ophiolites are distributed along the Alpine-Himalayan Orogenic Belt (AHOB; Figure 1). The Eocene ophiolites occur along the Iran-Iraq border from Kermanshah (Iran;

Moghadam and Stern, 2015) to Hasanbag (Iraq; Ali et al., 2013). The Eocene and younger ophiolites occur in southeastern Asia, e.g., in Indonesia (Ishikawa et al., 2007), Philippines (Yumul, 2007), Taiwan (Jahn, 1986), Japan (Hirano et al., 2003) and western South America in Chile (Veloso et al., 2005).

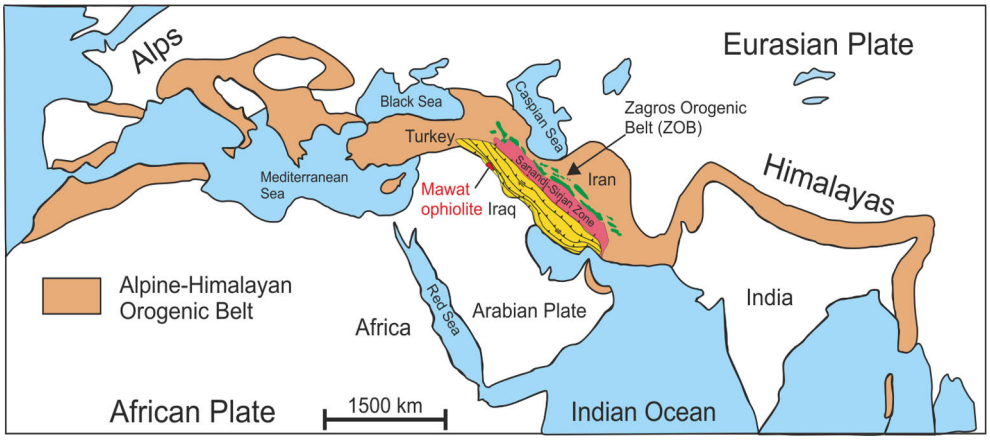

Figure 1. Tectonic map showing the geographic extent of the Alpine-Himalayan Orogenic Belt (AHOB), the location of the Mawat ophiolite and the Zagros Thrust Zone Zone (yellow) are indicated (modified after Furnes et al. 2020).

Collision between the continents of Eurasia and Gondwana caused the closure of the Tethyan ocean producing the Tethyan ophiolite belt that extends from the Balkan Peninsula through the Anatolian Taurus Mountains to the Iraqi-Iranian Zagros Mountains (Dilek et al., 2007). The Zagros Orogenic Belt (ZOB; Figure 1) is part of the AHOB and extends ~ 2000 km from southeastern Turkey, northern Syria and and northeastern Iraq to western and southern Iran. The ZOB formed in three major tectonic events: a) early to late Cretaceous subduction of the Neotethyan oceanic plate beneath the Eurasian continental plate, b) emplacement of the Late Cretaceous Neotethyan ophiolites on the Arabian passive continental margin, and c) the Cenozoic collision of the Arabian and Eurasian continental plates (Alavi, 1994; Agard et al., 2995; Mohajjel and Fergusson, 2014; Moghadam and Stern, 2014; Moghadam et al., 2019).

1.2 Zagros Orogenic Belt

The ZOB formed in a young continental convergence and provides an opportunity to assess the tectonic cycle processes of subduction, obduction and continental collision. The ZOB is in an intermediate phase between the preliminary obduction preserved along the Makran-Oman transect and the late-stage collision observed in

southern Turkey (Agard et al., 2005; Moghadam et al., 2014; Fergusson et al., 2016).The Neotethyan ophiolites along the ZOB are emplaced in two belts (Stöcklin, 1977; Homke et al., 2010; Ghazi et al., 2012). The Inner and Outer Ophiolitic Zagros Belts are separated by the Sanandaj-Sirjan metamorphic terrane. The Inner Zagros Ophiolitic Belt is located between the Sanandaj-Sirjan and Central Iran, comprising the Khoy, Nain, Dehshir, Shahr-e-Babak and Baft ophiolites (Moghadam and Stern, 2011). The Outer Zagros Ophiolitic Belt is located between the Sanandaj-Sirjan and Zagros Thrust Zones (Figure 1), and contains the Iraqi ophiolites Hasanbag, Pushtashan, Bulfat, Mawat and Penjwen, as well as the Iranian ophiolites Piranshahr, Kermanshah, Neyriz and Haji Abad ophiolites (Sahfaii Moghadam and Stern, 2011; Ali et al., 2016; Ismail et al., 2017).

1.3 Ophiolites in northeast Iraq

The Iraqi ophiolites are allochthons, derived from the Neotethyan ocean that started to form in the late Permian to early Triassic by rifting of the northern part of Gondwana (Agard et al., 2005). These ophiolites were emplaced in two episodes in the late Cretaceous and Paleogene (Ismail et al., 2014). They formed in a new subduction zone that was initiated on the southern part of Eurasia (Moghadam and Stern, 2011).The Iraqi ophiolites, which crop out along the Iraqi Zagros Suture Zone (IZSZ; Figure 2), are distributed discontinuously and record the ongoing collision sites: **a)** between the Arabian continent and the Iranian microcontinent, northeastern Iraq and **b)** between the Arabian and Turkish continents in northern Iraq (Numan, 1997). The IZSZ consists of two allochthonous units: the upper and lower units (Jassim and Goff, 2006) subdivided into three tectonic sub-zones: the Qulqula-Khwakurk, the Penjwen-Walsh, and the Shalair (Buday and Jassim, 1987; Jassim and Goff, 2006; Figure 2). The Penjwen-Walsh is consists of two thrust sheets. The lower allochthon is the Eocene-Oligocene Walash-Naopurdan Group made up of volcanic-sedimentary arc rocks (Ali et al., 2013) and the upper allochthon is the Cretaceous Gimo-Qandil Group which is the ophiolite-bearing terrane (Ali et al., 2012). It contains the Cretaceous ophiolites and suprasubduction zone assemblages, e.g., the Penjwen, Mawat, Pushtashan, Hasanbag and Kata-Rash ophiolites (Aswad et al., 2012; 2016, 2019; Ismail et al., 2014, 2017, 2020; Abdulla, 2015). The lower allochthon contains incomplete fragments of mélange-type ophiolites, e.g., Rayat (Arai et al., 2006; Ismail et al., 2009, 2010, 2014; Ali et al., 2019), Qalander (Ismail and Al-Chalabi, 2006) and Bulfat (Ali et al. 2017) were identified as Cenozoic ophiolites now preserved as fragments in the Paleogene Wlash-Naupordan groups.

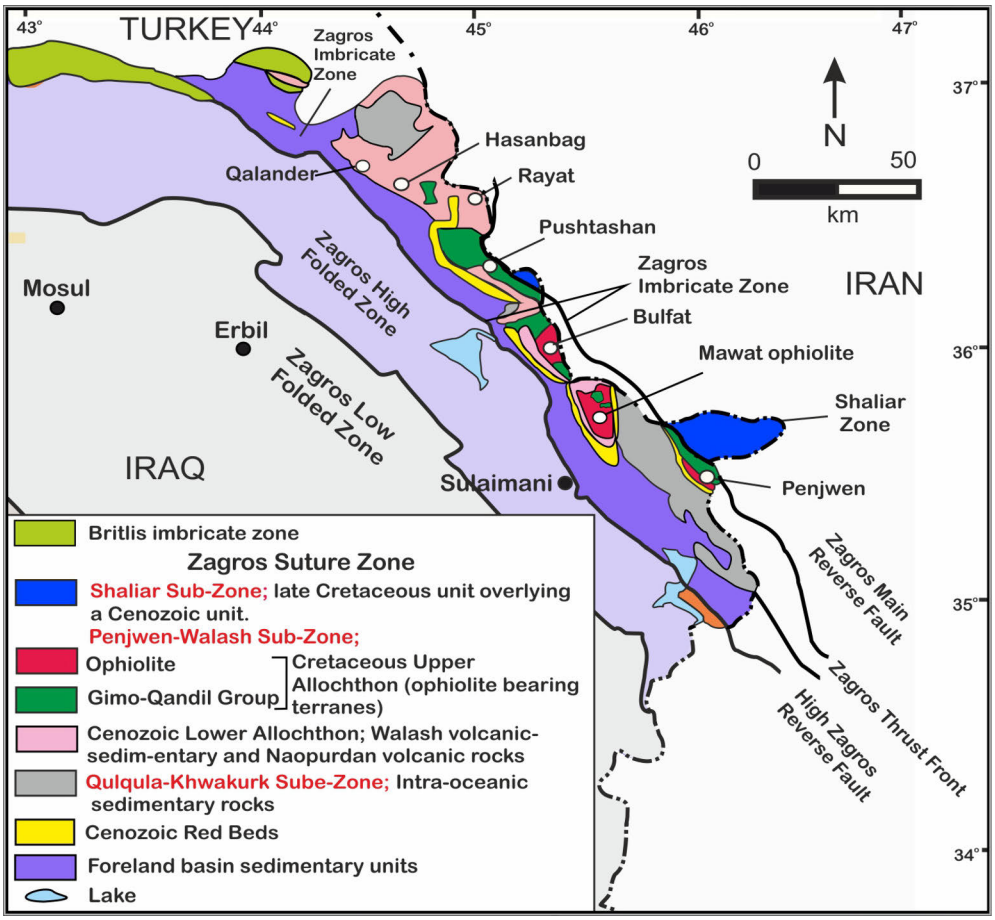

Figure 2. Regional tectonic map of northeastern Iraq Kurdistan region showing the major tectonic subdivisions in the Iraqi Zagros Suture Zone, modified after Al-Kadhimi et al. (1996). Tectonic zones and boundaries, modified after Al-Qayim et al. (2012).

1.4 Objectives of the study

The aim of this study is to elucidate the evolution and geotectonic environment of the mantle-derived rocks in the Mawat ophiolite (MO) in northeastern Iraq. The thesis describes a) the petrographic features, b) whole-rock geochemical composition of ultramafic, mafic and felsic rocks, c) U-Pb monazite and zircon dating of two felsic dykes and a gabbro, and d) Hf zircon isotope composition from two felsic dykes and a gabbro from the MO.

Paper I is preliminary based on field observations, to identify the different rock units in the MO. Four samples from two felsic dykes and a gabbro were collected from the eastern part of the MO for the U–Pb zircon and monazite dating and the Lu–Hf isotope analysis. The new findings of the age determinations are used to

interpret the tectonic setting of the ophiolite and the initial ε_{Hf} values are used to discuss the magma sources of the rock types.

Paper II describes the petrography, mineralogy and geochemistry of eight felsic dykes in the eastern part of the MO. The purpose is to discuss their magma sources and regions. The findings are discussed in comparison with the previous works reported on the felsic rocks in the western and central parts of the MO.

Paper III describes the petrography and geochemistry of the mafic and ultramafic rocks. The purpose of the study is to present the petrographic and geochemical characteristics and discuss the origin and tectonic setting of the MO. Thirty-two mafic and ultramafic samples were selected for geochemical analyses. Thirteen samples of both types were re-analysed with a method with lower detection limits.

2 Study area

2.1 Mawat ophiolite

The MO crops out on over ~250 km^2 (Jassim, 1973; Al-Mehaidi, 1975) in an elevated and rough topographic area northeast of the city of Sulaimani, northeastern Iraq. The lithostratigraphic sequence is relatively preserved, complete and consists of mantle and crustal sections as the main components. Minor diabasic dykes, dioritic lenses and felsic dykes intruded the mafic and ultramafic rocks. The mantle section consists of peridotite, serpentinized harzburgite, dunite, pyroxenitic dykes, chromitite and minor lherzolite. The crustal section comprises layered gabbro, amphibole-rich gabbros as well as basalts and siliceous carbonates. The volcanic rocks occur in lower metavolcanic unit (Mawat group) and the upper volcano-sedimentary unit (Gimo group) and they are exposed in the northern and southern parts of the MO (Figure 3).

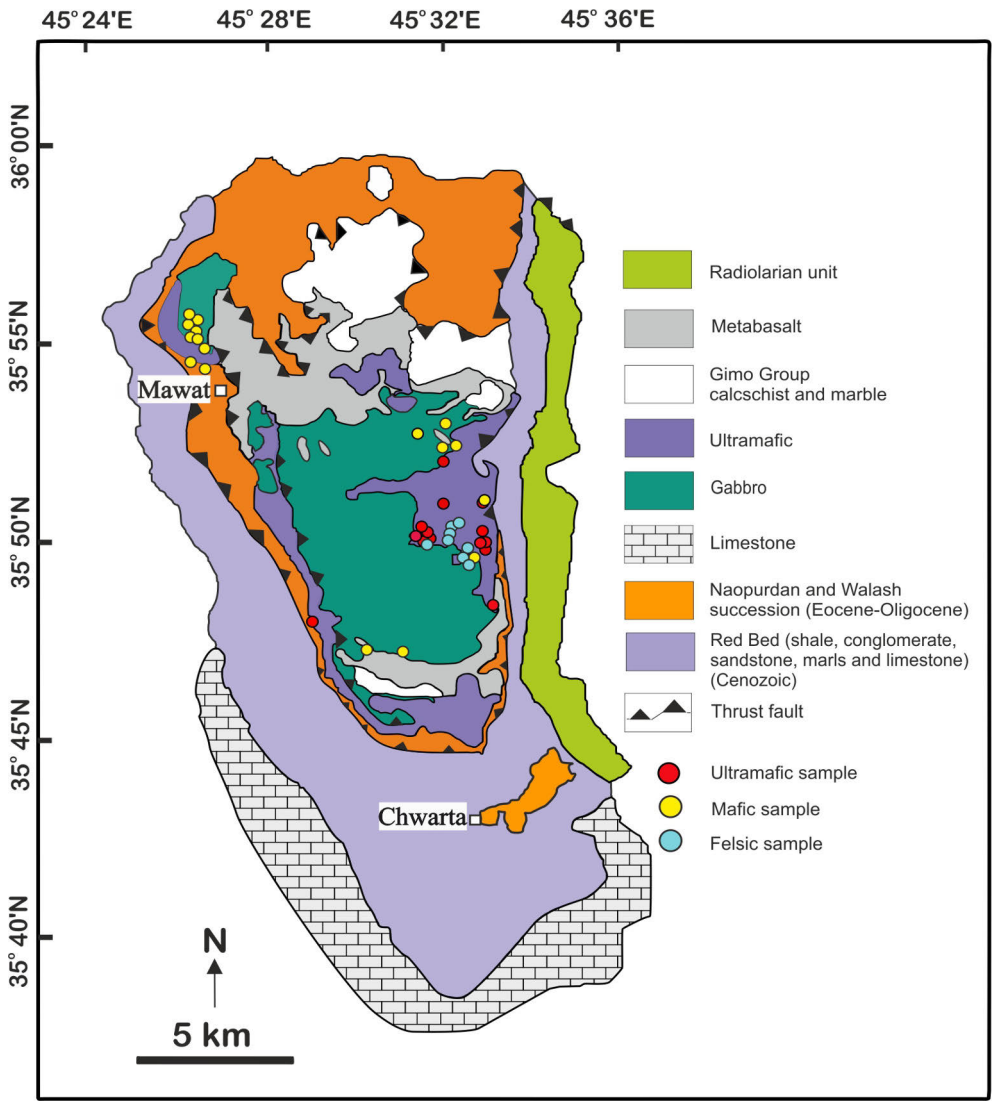

Figure 3. Simplified geological map of the Mawat ophiolite, showing locations of felsic samples (Paper I-II) and mafic and ultrmafic samples (Paper III), modified after Aziz (2008).

These rock units are deformed and they are mixed with sediments on the top and are covered by soils. Thus, the contact relationships are difficult to observe. The topography of the MO is elevated, with high relief hampering to reach the key outcrops. Previous studies on the mafic rocks conclude that these have MORB affinity (Mirza and Ismail, 2007). In the southern part of the MO, the metagabbros are tholeiitic MORBs formed by partial melting of peridotite (Koyi et al., 2010). Azizi et al. (2013) proposed that the Mawat magmatism shows an OIB affinity and suggested that it is related to a plume setting.

3 Materials and Methods

3.1 Field work and sample preparation

The high and rugged topography caused that the outcrops were sometimes hard to reach. The sample locations were positioned with GPS and their location are shown in Figure 3. More than 80 bedrock observations were made and 85 rock samples were collected. The samples selected for the study are split in three pieces: a) whole rock geochemistry, b) thin sectin preparation, and c) zircon and monazite separation for the U-Pb dating and Lu-Hf isotope analysis.

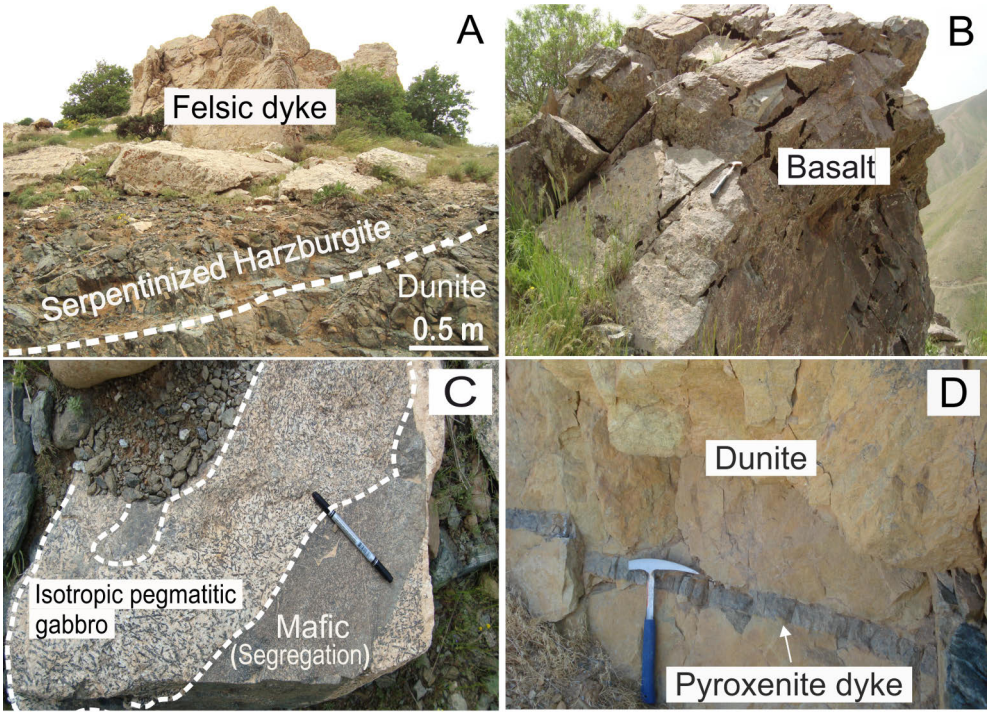

Figure 4. Field photographs for the studied areas. A) Felsic dyke crosscutting the mantle peridotite (serpentinized harzburgite), B) Fine-grained basalt, C) Isotropic gabbro and fine-grained mafic segregation, D) Massive block of dunite was cut by pyroxenite dyke.

3.2 Petrography

Polished and glass-covered thin sections as well as polished thick section were prepared at the thin section facilities at the Geohouse, University of Turku. A second batch (n=30) of polished thin section were prepared in commercial Lab Vanpetro in Vancouver Petrographics Ltd. Canada. Mineral identification was done by optical microscopy. The identification of the zircons, monazites and xenotimes was done from the epoxy mounts. Furthermore, two analytical methods were used to support the mineral identification. First, the element mapping was done with Bruker M4 Tornado micro-XRF facility equipped with two SDD detectors at the University of Turku, Finland. Second, a more detailed mineral identification with point analysis was performed in the Finnish Geosciences Research Laboratory at the Geological Survey of Finland, Espoo with Hitachi SU3900 Scanning Electron Microscope (SEM).

3.3 Whole rock geochemistry

The samples were cut into small pieces by a diamond saw. Part of the samples were used to prepare the polished thin or thick sections and isotope analysis, while a jaw crusher crushed the remains.

A total of forty-eight rock samples were analysed for whole rock geochemistry at Acme Analytical Laboratories Ltd. (Acme) in Vancouver, Canada (Paper II-III). Major elements were analysed by inductively coupled plasma-emission spectrometry (ICP-OES) with Spectro Ciros Vision instrument. The trace elements were analysed by inductively coupled plasma-mass spectrometry (ICP-MS) with PerkinElmer ELAN 9000 instrument. The data are interpreted and plotted with the GCDKit software (Janousek et al., 2006). Four rock samples were used for the geochronology and Lu-Hf studies.

Thirteen samples from the mafic and ultramafic rocks were re-analysed at Acme Analytical Laboratories Ltd. in Peth, Australia (Paper III). The samples were crushed and pulverised in a mild steel grinder mill. The major elements were analysed by X-Ray Fluorescence Spectrometry (XRF) on oven dry (105°C) samples. The trace elements were analysed by Laser ablation inductively coupled plasma-mass spectrometry (ICP-MS).

3.4 Zircon and monazite U-Pb dating

Four samples from two felsic dykes and a gabbro were selected for the monazite and zircon separation. The separation process was done through standard procedure including crushing, grinding, panning, magnetic separation, heavy liquid separation and hand packing. The zircon and monazite grains were mounted in the epoxy resin,

cut to half and polished. The Back-scattered Electron (BSE) images were conducted using LEO 1530 Gemini scanning electron microscope at Åbo Akademi University, Finland and JEOL JSM-7100F FE-SEM Schottky attached to an Oxford Instruments energy dispersive spectrometer (EDS) X-max (80 mm2) in the Finnish Geosciences Research Laboratory at the Geological Survey of Finland in Espoo.

The U-Pb analyses were performed with two instruments: the first was Nu Plasma HR multicollector ICP-MS at the geological Survey of Finland in Espoo using a technique very similar to Rosa et al. (2009), except that a Photon Machine Analyte G2 laser microprobe was used. The second was performed using Nu AttoM single collector ICP-MS at Geological Survey of Finald, Espoo connected to a photon Machine Ecite laser ablation system

The calibration standard zircon GJ-1 (609 ±1 Ma; Belousova et al., 2006), PL (337± 0.4 Ma; Sláma et al., 2007) and in-house standard A382 (1877 ± 2 Ma, Huhma et al., 2012), and the calibration standard monazite 44069 (424 ± 1 Ma; Aleinikoff et al., 2006) or in-house standard 117531 (272 ± 4 Ma) were run at the beginning and end of each analytical session and at regular intervals during sessions. Plotting of the U-Pb isotopic data and age calculations were performed using the Isoplot/Ex 4.15 program (Ludwig, 2003).

3.5 Zircon Lu-Hf analysis

The zircon Hf isotope analyses were performed on the same or ajacent domains of the grains on which the U-Pb dating was done. The analyses were carried out using the Nu Plasma HR multicollector ICP-MS at the geological Survey of Finland in Espoo using a technique very similar to Heinonen et al. (2010) except that a Photon Machine Analyte G2 laser ablation system was used. The zircon standard GJ-1 was run at frequent intervals for quality control. Multiple LA-MC-ICP-MS analyses of GJ-1 during the course of the present study yielded a $^{176}Hf/^{177}Hf$ of 0.28194 ± 6 (1σ, n=35), which is just within the error of the results obtained by solution MC-ICP-MS analyses for GJ-1 (0.281998 ± 7, Gerdes and Zeh 2006; 0.282000 ± 5, Morel et al., 2008). For the calculation of ε_{Hf} values, present-day chondritic $^{176}Hf/^{177}Hf$ = 0.282785 and $^{176}Lu/^{177}Hf$ = 0.0336 were used (Bouvier et al., 2008).

4 Results

4.1 U-Pb monazite and zircon ages

Three felsic samples were analysed for the U-Pb zircon and monazite and a gabbro sample for the U-Pb zircon. The zircon textures from the felsic samples display spongy domains and intergrowth of xenotime, monazite and unidentied Th- and U-rich phases. The monazite textures show inclusions of xentime, thorite and zircon, and dark and bright spots. Zircons textures from the gabbro show weak internal zoning and contains plagioclase inclusions.

The felsic rocks show crystallisation age of monazite at 94.6 ± 1.2 Ma. The gabbro sample show ages varing between 81.2 ± 2.5 Ma and 38 Ma.

4.2 Lu-Hf isotope

The zircon Hf isotopes were analysed for two felsic samples and a gabbro. The zircon of the felsic sample D1a show $^{206}Pb/^{238}U$ ages spreading between 100 and 78 Ma. The initial ε_{Hf} values range between -10 and +2.2 with an average value of -2.7. Two zircons from the second felsic sample D3 were used to calculte the initial ε_{Hf} values for $^{206}Pb/^{238}U$ ages (83 and 70 Ma). The initial ε_{Hf} values range between - 4.4 and - 1.7 with an average value of -3.1.

For the gabbro, the individual zircon $^{206}Pb/^{238}U$ ages between 75 and 40 Ma were used for the Hf measurements. The initial ε_{Hf} values range between - 3.3 and + 9.1 with an average value of + 3.5.

4.3 Whole rock geochemistry

The samples range in composition from felsic to mafic and ultramafic. Based on the petrography, the felsic dykes are classified into two types: the tonalities and granites. In the Total Alkalis vs. Silica diagram, both types fall in the granite fields except for two samples from tonalite type that plot in the quartz-monzonite-synite field. The tonalite and granites types show differences in major and trace elements indicating that they come from different sources but are partially mixed. Geochemically, the mafic samples (basalts and gabbros) show a distinctive differences in the major, trace

elements and REE patterns suggesting different tectonic settings. The ultramafic samples of dunites and serpentinites and pyroxenites are highly depleted in the LILEs and most of the HFSEs. They plot in two patterns below the MORB-line reference and both show a boninite affinity.

4.4 Review

4.4.1 Paper I

This study display the U-Pb, Lu-Hf isotope analyses data from felsic dykes and gabbro from the eastern part of the MO. The monazites from the felsic dykes yield an age of 94.6 ± 1.2 Ma which is interpreted as a crystallization age of the dykes. The zircons from felsic dykes yield range of ages from 222 Ma to 46 Ma because of the Pb mobility. The zircon from the gabbro yield a wide range of ages from 81 to 38 Ma and the oldest one reflects the crystallization age of the magma.

The two felsic dykes (zircon ages between 100 and 78 Ma, and 83 and 70 Ma, respectively) have negative initial ε_{Hf} values of - 2.7 and - 3.1, respectively. These negative values indicate that the source of the felsic magma is older than the intrusion age suggesting a crustal contribution. The zircon grains from the gabbro have a positive average initial ε_{Hf} value of +3.5 with the highest value of + 9.1. That suggest the magma was derived from a juvenile source.

4.4.2 Paper II

This publication presents whole-rock major and trace elements as well as REE patterns of eight felsic dykes in the eastern MO. The felsic dykes in the western, central and eastern parts of the MO occur in two compositional groups; tonalites and granites. The eastern tonalite dykes are composed of plagioclase, amphibole, and quartz and they are weakly peraluminous to metaluminous, low in K_2O and TiO_2 and high in Na_2O. The eastern granite dykes are composed of K-feldspar, quartz, plagioclase, muscovite and biotite and they are strongly peraluminous with moderate to high K_2O and Na_2O and very low TiO_2.

The western tonalite dykes show high Sr/Y ratios, high MgO and Ni contents resembling the adakite melts derived from subducted oceanic crust contaminated by mantle wedge peridotites. The central granite dykes were derived from a sedimentary source. The eastern dykes include both tonalites and granites and they are mixed with each other in various proportions. They have intermediate compositions between the western and central dykes. The eastern tonalites have low MgO, Cr and Ni contents and lower Sr/Y compared to the western ones. They are interpreted to be formed by hornblende and plagioclase fractionation in a shallow-level magma

chamber. Hornblende fractionation is also suggested as responsible for low Mg, Cr and Ni contents in the granites. The eastern granites are high in K_2O, Rb, and LREEs and are derived from subducted sediments.

4.4.3 Paper III

In this manuscript, the whole-rock major and trace elements and REE patterns of the mafic (basalts and gabbros) and ultramafic (dunite and serpentinite with pyroxenite) rocks are described. The data show that the basaltic rocks are tholeiitic, characterized by depletion of LREEs and display a positive trend from LREE to HREE with low Ti/V ratios. The gabbroic rocks are mostly calc-alkaline, characterized by enrichment of LREE with a negative REE trend and high Ti/V ratios. The basalts and ultramafic samples are highly depleted in the LILEs and most of the HFSEs and plot below the N-MORB reference line suggesting that these elements have been mobile. The immobile element diagrams show that the basaltic and ultramafic rocks resemble the boninitic lavas related to subduction initiation. This is confirmed with the Ti/V diagram, where the rocks fall in the boninite field. The gabbroic rocks plot in the MORB field of Ti/V diagram. This is interpreted as an indication of later rifting during the extensional setting above a subduction zone. In the Th/Yb vs. Nb/Yb diagram, the mafic rocks of this study and the reference data from other parts of the MO are classified into three groups. They plot in the oceanic arc, continental arc and MORB fields. In the Ti/V diagrams, they fall in the MORB, IAT and boninte fields. These geochemical data are consistent with the suprasubduction zone tectonic setting.

5 Discussion

5.1 Ages of the felsic dykes and gabbro

The felsic dykes from the MO have crystallized at ~ 95 Ma (Paper I). That age is in good agreement with pervious age determinations from the Daraban leucogranite in the MO (96.8 ± 6. Ma zircon; 93.2 ± 1.7 Ma monazite and 94.6 ± 6.6 Ma xenotime; Mohammad and Qaradaghi, 2016; Mohammad et al., 2017), the Rb-Sr mineral isochron age of 93.4 ± 1.8 Ma (Aziz et al., 2013) and the nearby 96 ± 2 Ma Pushtashan trondhjemite and the 90.74 ± 0.56 Ma Penjwen trondhjemite (zircon; Ismail et al., 2017; 2020). Similar ages are aslo common throughout the Neotethyan ophiolites (e.g., Moghadam and Stern, 2011).

We interpret the oldest 81 Ma age to show the crystallization age of the zircon and the gabbro magma. Similar 79.3 ± 0.9 Ma age for gabbroic magmatism is common in the Kermanshah ophiolite, (~ 250 km southeast MO). Ao et al., (2016) interpret the gabbro to be related to continental rifting forming the oceanic crust. The gabbro of the MO is interpreted as rift-related above the suprasubduction zone.

A specific feature of the U-Pb data sets in both felsic and mafic samples is the wide range of zircon and monazite ages. The youngest ages in all three samples are ~ 40 Ma which we interpret as the time of Pb loss/mobilisation event. There are many igneous rocks of that age nearby the MO, such as the 39 Ma gabbro in Bulfat ophiolite, ~ 50 km north Mawat, (Ali et al., 2017). ^{40}Ar -^{39}Ar hornblende and biotite also give an age of 39 Ma indicating a rapid cooling at the time (Aswad et al., 2016). In the Kermanshah ophiolite ~ 250 km southeast MO, there are a 39 Ma gabbro and a 36 Ma plagiogranite (Ao et al., 2016), and 41-39 Ma granites occur in the northern part of Sanandaj-Sirjan zone (Zhang et al., 2018).

The ~ 40 Ma ages recorded in Mawat are probably related to these tectonic events even though they are still are poorly known and controversial in detail. During the closure of the Neotethyan ocean the crustal extension and related volcanism took place at 50-40 Ma in southern Turkey (Robertson et al., 2013). In Iran, extensional events are evidenced in the late Paleocene to late Eocene 54-40 Ma volcanism and plutonism (Verdel et al., 2011).

In the MO, the c. 97 Ma Daraban felsic dyke (Mohammad and Qaradaghi, 2016) has its ^{40}Ar-^{39}Ar muscovite age 38 Ma (Mohammad et al., 2014). This is interpreted to

represent the beginning of the continental collision between the Arabian and Eurasian continents. Same conclusion was drawn from similar ^{40}Ar-^{39}Ar ages from the Bulfat ophiolite (Aswad et al, 2016). Perhaps the advancing and retreating subduction generated both compressional and extensional events.

5.2 Lu-Hf data

The negative average initial ε_{Hf} values for the felsic dykes are -2.7 and -3.1 with the lowest value of -10.0 (Paper I). Such negative values indicate that the source of the felsic magma is older than the intrusion age suggesting a crustal contribution. The wide range of values indicates a heterogeneous or mixed source, or alternatively later incomplete equilibration.The gabbro has a positive average initial value of +3.5 with the highest value of + 9.1, suggesting that the magma was derived from a juvenile source. The average initial ε_{Hf} value in the nearby Pushtashan ophiolite is higher +13.9 (Ismail et al., 2017). This may indicate that the MO gabbro comes from a slightly older source or it has contaminated with such a source.

5.3 Magma sources of the felsic dykes

Since the felsic rocks are classified into two groups, tonalites and granites, their magma sources probably are different. The Rb/Sr vs. Rb/Ba diagram differentiates the magma sources and suggests that the tonalite and granite derive from mafic and sedimentary sources, respectively. The low contents of K_2O and Rb, in particular, support a mafic source for the tonalite (Rollinson, 2014). The high K, Pb, Th, U and Pb in the granite along with the aluminous mineralogy suggests that they formed through partial melting of metasediments (Cox et al., 1999; Rollinson, 2014; Haase et al., 2015).

The MO tonalites, characterized by low K_2O and Rb contents, are interpreted to derive from a mafic source (see Rollinson, 2014). These are consistent with compositions from the eastern and western tonalites. Also, the low to high La/Sm ratio for given La concetrations implies that these trace elements are more likely controlled by partial melting rather than fractional crystallization.

In the Zr vs. Y diagram, the eastern and western tonalites plot in the field of anatectic melting of a mafic source (Pedersen and Malpas, 1984). This may suggest that sediment-derived melts were also partially involved.

The zircon ε_{Hf} data from the eastern tonalite sample show a range of negative values (-4.4 to -1.7; Paper I). The negative ε_{Hf} values require an additional component of non-radiogenic Hf to be present in the magmas, which strongly points to continental material (Griffin et al., 2000). Hf isotope composition thus indicates that the eastern tonalites were likely derived from mixed sources or were

contaminated with sediments.The western tonalite show an adakite signature in terms of Sr and Y concentrations and ratios. They also have high MgO, Mg#, Ni, and V contents, suggesting that they were contaminated with the mantle wedge (Rollison, 2014). Such features are consistent with adakitic melts derived from subducted oceanic slab (Defant and Drummond, 1990; Martin 1999).

The eastern tonalites have low Y and Yb but Sr contents are lower than in the western tonalites. The Sr/Y straddle the adakite/volcanic arc boundary. The eastern tonalites are derived from mixtures of mafic and felsic magmas. The low-Sr sedimentary components may have lowered the originally higher Sr/Y ratios. The eastern rocks have low MgO, Ni, Co and V contents and negligible Cr. The Mg# are similar in both locations. We interpret that the eastern tonalite magma fractionated in a shallow-level andesitic magma chamber, because hornblende has very high K_D for Co, Cr, Ni and V in such a magma (Rollinson, 1993) and fractionated together with plagioclase (Moyen, 2009). Low concentration of these elements therefore are related to hornblende (+ plagioclase) removal.

5.4 Petrogenesis and tectonic setting of the mafic and ultamafic rocks

The basaltic rocks are slightly enriched in the HREEs relative to LREEs with positive Ba, U, K, Pb and Sr and negative Nb, Zr and Ti anomalies. The N-MORB normalized diagram suggests that the basalts formed by partial melting of a depleted mantle. These features resemble those of the boninites formed in a forearc setting related to initial intra-oceanic subduction settings (Shervais et al., 2019).

Based on the Sm/Lu vs Sr/Ce diagram, the basaltic rocks show higher degree of partial melting relative to the gabbros (Fig.9a in Paper III) and the La/Yb vs. La confirms the results show that both the gabbro and basalts follow the partial melting trend and the basalts have higher degree of partial melting than the gabbros (Fig. 9b in Paper III).

The values of Ce/Yb (0.08–0.2) and LaN/YbN (0.22–0.49) in the basalts are lower than those in the gabbros (1.18–2.7 and 3.9–10.3, respectively). This suggests that the basalts formed by higher degree of partial melting of a depleted-mantle source compared to the gabbros that formed by low degree of partial melting of an enriched mantle source (Saccani et al., 2003).

The ultramafic samples are slightly enriched in the LREEs compared to MREEs and HREEs, showing a spoon-shaped pattern with extremely low ΣREEs. Both the dunite/serpentinites and the pyroxenites plot below the N-MORB reference line. The N-MORB and primitive mantle-normalized multi-element diagrams show that there are two pattern types: the first type is the dunite and serpentinite group which are extremely depleted in the LILEs and most of the HFS elements. The second type is

the pyroxenite group which is less depleted in the LILE and some HFS elements compared to the dunite/serpentinite group. The ultramafic samples show positive U, Pb and La and negative Nb, Ta and Zr anomalies. These features suggest that their parental magmas are derived from highly depleted mantle and partial melting is the main process in their formation (Fig. 8g; Paper III).

Geochemical compositions, especially the trace elements, are an effective tool to infer the tectonic setting of the ophiolites. In this study we use the Nb/Y vs. Zr/Ti (Pearce, 1996) for classification purposes, Nb/Yb vs. Th/Yb diagram (Pearce, 2008) to separate the subduction-unrelated ophiolites from the subduction-related ophiolites and Nb_N vs. Th_N diagram (Sccani, 2015) to identify the forearc basalts. These diagrams are based on the immobile elements to minimise the effect of alteration.

A general view of the tectonic setting of the mafic rocks is determined by the Th/Yb vs. Nb/Yb diagram (Pearce, 2008). It shows that the mafic rocks fall above the MORB-OIB array. The basaltic rocks fall in the oceanic arc field and the gabbros in the continental arc field. The data that fall above the MORB-OIB array is explained by variable enrichment of elements transported by hydrous fluids with or without melts released from subducted oceanic slab. This suggests a subduction-related tectonic setting (Furnes et al, 2020).

The Ti/1000 vs. V diagram discriminates the magmas of boninites, island-arcs, MORBs and alkali basalts. The ultramafic and basaltic samples plot in the boninite field. The gabbroic samples plot in the MORB field. The mafic rocks from the western and central parts from the MO (Mirza and Ismail, 2007; Azizi et al. 2013) plot in the boninite-IAT fields, while the mafic rocks from Kermanshah plot in IAT and MORB/BABB-OIB fields (Fig. 11b in Paper III).

The Nb_N vs. Th_N diagram shows that the basaltic samples and the mafic rocks from the western MO and six mafic rocks from the Kermanshah ophiolite plot within the intra-oceanic system and forearc. The majority of the mafic rocks from the central MO and four rocks from the Kermanshah ophiolite fall within the backarc field. The gabbros and one mafic rock from the central MO and two mafic rocks from the Kermanshah ophiolite fall within the continental arc field (Fig, 11c: Paper III).

The mafic rocks have boninite, IAT and MORB-like compositions. Therefore, these rocks (MORB, IAT and boninites) formed in the same forearc region, probably with early MORB-like (Reagan et al., 2010) and younger boninitic lavas, as is common for forearc settings (Dilek & Furnes, 2014; Ishizuka et al., 2014). This is, however, difficult to prove in the MO because the stratigraphic order is disrupted by thrusting and now the ultramafic (harzburgite and dunite) rocks are on the top, the amphibole-gabbros are in the middle and the basalts are at the bottom.

The basalts and gabbros were derived from different sources. The basalts are slightly enriched in HREEs related to LREEs, with positive Ba, U, Pb, and Sr anomalies (Fig. 9d; Paper III) indicating that they were produced by partial melting of the depleted mantle peridotite. These features are similar to boninites formed in a forearc setting related to the intra-oceanic initial subduction (Shervais et al., 2019). The gabbros are interpreted as rift-related in an extensional setting above the sibduction zone setting >15 Ma later that the basalts and ultramafic rocks.

6 Summary/Conclusions

The thesis describes the evolution of the mantle-derived magmas and their temporally and spatially associated changes during the late Cretaceous-Eocene. The zircon U-Pb dating results give ages between 222 and 38 Ma interpreted to be related to radiogenic Pb mobility and Pb loss. The thesis describes the evolution of the mantle-derived magmas and their temporally and spatially associated changes during the late Cretaceous-Eocene. The monazite 94.6 ± 1.2 Ma age is considered as the crystallization age of the felsic dykes and the oldest zircons in gabbro provide the age of 81.2 ± 2.5 Ma which is the crystallization age of the gabbro and interpreted to be related to rifting above the suparsubduction zone. The youngest ages ~ 40 Ma are related to crustal extension. The negative initial ε_{Hf} values for felsic dykes indicate that the magma comes from an older source. The positive initial ε_{Hf} values for the gabbro suggest that the magma comes from a juvenile source. The felsic dykes occur in two types: tonalites and granites. The dykes also occur in the western part as a plagiogranites and central part as a leucogranites. Both types are mixed in various proportions in the east part of the MO. The eastern tonalites are weakly peraluminous to metaluminous and are low in K_2O, TiO_2, and high in Na_2O. They have low MgO, Cr, and Ni contents and low Sr/Y compared to the western ones where these are high and similar to adakites. These were derived from partial melting of the subducted oceanic slab. The eastern tonalites underwent hornblende and plagioclase fractionation in a shallow-level magma chamber modifying their original compositions. The eastern granites are strongly peraluminous, moderate to high in K_2O, Pb and Na_2O, and very low in TiO_2. Their melts are derived from psammitic sediments on the top of the subducted slab. Parental melts of the tonalities and granites partially mixed in shallow magma chambers in east.

The basalts and the ultramafic rocks are extremely depleted in the LILE and some HFSE elements. They plot below the N-MORB reference line suggesting that these elements have been mobile. The basaltic and ultramafic rocks resemble the arc boninites related to the subduction initiation setting. This is confirmed with Ti/1000 vs. V diagram. This suggests that these rocks formed in the same forearc region. The undepleted pattern of the gabbros plot parallel to the N-MORB reference line and within the MORB field in the V vs. Ti/1000 diagram. This is an indication of rifting

in an extensional setting above the subduction zone. The geochemical data is consistent with the tectonic setting for suprasubduction zone ophiolite.

Acknowledgemets

First of all, I would like to express my deepest gratitude to my principal supervisor Markku Väisänen for his guidance, patience and motivation through all these years. I admire his knowledge, enthusiasm and tenacity. I am thankful for that and for sharing some of knowledge with me. His support and patience helped me on the way to the first step to the scientific research. It would be too difficult to finish my dissertation without him.

I express my deep gratitude to my co-supervisor Sabah A. Ismail for his continuous guidance and encouragement and urging to overcome difficulties. I thank him for his role in sharing his knowledge for a deep understanding of the studied area and for his role in facilitating fieldwork and sampling to overcome risks. I would also like to acknowledge the Department of Geography and Geology for supporting and providing the Lab equipment needed to complete my dissertation.

I would like to thank the Finnish Geosciences Research Laboratory and all my co-authors who work in the Geological Survey of Finland in Espoo, Hugh O'Brien, Yann Lahaye, Marja Lehtonen and Bo Johanson. I like to thank Arto Peltola for the technical support in the laboratory. He was always ready to give a help. Warm thanks go to Timo Kilpeläinen, Eila Hietaharju, Timo Saarinen and Pietari Skyttä the helps and advices. Speacial thanks to my office mates Evgenia Salin and Jaakko Kara as they were always willing to help and give the best suggestions. Special thanks go to Prof. Dr. Yawooz Kettanah, for help and continuous encouragement. Acknowledgments go to amazing long friendships with Hazem, Qassim, Amjad, and others as they helped and supported me in this journey.

I cannot forget the role of my beloved wife Sahar, as she understood the situation and surrounded me with love, encouragement, patience and continued to fill my sky with her supplication. All gratitude, thanks and love for her. Thanks to my beloved children Amani, Ali, Hadi and Lilia as they have endured some of my annoyance and a lack of patience. But their existence and love keep me going.

Speacial thank go to my father, as he wished me the best. Thanks to my brothers and sisters, as they all the times support, encourage and to those who wished me success.

Thank the University of Babylon, College of Science, and Department of Applied Geology to give me this opportunity to complete my doctoral studies. Thanks to the Ministry of Higher Education and Scientific Research of Iraq for the financial support during this thesis project. Thanks to the Iraq Geological Survey (GEOSURV) for the field work assistant.

Finally, Praise be to Allah, Lord of the worlds, and many blessings and peace be upon the best messengers.

06.08.2021
Heider Al Humadi

List of References

Agard, P., Omrani, J., Jolivet, L., & Mouthereau, F. 2005. Convergence history across Zagros (Iran): constraints from collisional and earlier deformation. *International Journal of Earth Sciences*, 94(3), p. 401–419.

Alavi, M. 1994. Tectonics of the Zagros orogenic belt of Iran: new data and interpretations. *Tectonophysics*, 229(3-4), p. 211–238.

Aleinikoff, J. N., Schenck, W. S., Plank, M. O., Srogi, L., Fanning, C. M., Kamo, S. L., & Bosbyshell, H. 2006. Deciphering igneous and metamorphic events in high-grade rocks of the Wilmington Complex, Delaware: Morphology, cathodoluminescence and backscattered electron zoning, and SHRIMP U-Pb geochronology of zircon and monazite. *Geological Society of America Bulletin*, 118(1-2), p. 39–64.

Ali, S. A., Buckman, S., Aswad, K. J., Jones, B. G., Ismail, S. A., & Nutman, A. P. 2012. Recognition of Late Cretaceous Hasanbag ophiolite-arc rocks in the Kurdistan Region of the Iraqi Zagros suture zone: A missing link in the paleogeography of the closing Neotethys Ocean. *Lithosphere*, 4(5), p. 395–410.

Ali, S. A., Buckman, S., Aswad, K. J., Jones, B. G., Ismail, S. A., & Nutman, A. P. 2013. The tectonic evolution of a Neo-T ethyan (E ocene–O ligocene) island-arc (W alash and N aopurdan groups) in the Kurdistan region of the Northeast Iraqi Zagros Suture Zone. *Island Arc,* 22(1), p. 104–125.

Ali, S. A., Ismail, S. A., Nutman, A. P., Bennett, V. C., Jones, B. G., & Buckman, S. 2016. The intra-oceanic Cretaceous (~ 108 Ma) Kata–Rash arc fragment in the Kurdistan segment of Iraqi Zagros suture zone: Implications for Neotethys evolution and closure. *Lithos*, 260, p. 154–163.

Ali, S. A. 2017. 39 Ma U-Pb zircon age for the Shaki-Rash gabbro in the Bulfat igneous complex, Kurdistan region, Iraqi Zagros Suture zone: rifting of an Intra-Neotethys Cenozoic arc.*Ofioliti*, 42(2), p. 69–80

Ali, S. A., Nutman, A. P., Aswad, K. J., & Jones, B. G. 2019. Overview of the tectonic evolution of the Iraqi Zagros thrust zone: Sixty million years of Neotethyan ocean subduction. *Journal of Geodynamics*, 129, p. 162–177.

Al-Kadhimi, J.A.M., Sissakian, V.K., Fattah, A.S., Deikran, D.B., 1996. Tectonic Map of Iraq. Geological Survey and Mining of Iraq, p. 1–38

Al-Mehaidi, H. 1975. Tertiary nappe in Mawat range, NE Iraq. *Journal of the Geological Society of Iraq*, 5, p. 31–44.

Al-Qayim, B., Omer, A., & Koyi, H. 2012. Tectonostratigraphic overview of the Zagros suture zone, Kurdistan region, Northeast Iraq. GeoArabia, 17, p. 109–1

Anonymous. 1972. Penrose field conference on ophiolites. *Geotimes*, 17(12), p. 24–25.

Ao, S., Xiao, W., Jafari, M. K., Talebian, M., Chen, L., Wan, B., Ji, W., & Zhang, Z. 2016. U–Pb zircon ages, field geology and geochemistry of the Kermanshah ophiolite (Iran): From continental rifting at 79 Ma to oceanic core complex at ca. 36 Ma in the southern Neo-Tethys. *Gondwana Research*, 31, p. 305–318.

Arai, S., Shimizu, Y., Ismail, S. A., & Ahmed, A. H. 2006. Low-T formation of high-Cr spinel with apparently primary chemical characteristics within podiform chromitite from Rayat, northeastern Iraq. *Mineralogical Magazine*, 70(5), p. 499–508.

Aswad, K. J., Ali, S. A., Sheraefy, R. M. A., Nutman, A. P., Buckman, S., Jones, B. G., & Jourdan, F. 2016. $^{40}Ar/^{39}Ar$ hornblende and biotite geochronology of the Bulfat igneous complex, Zagros suture zone, NE Iraq: new insights on complexities of Paleogene arc magmatism during closure of the Neotethys Ocean. *Lithos*, 266, p. 406–413.

Aziz, N.R.H., 2008. Petrogenesis, Evolution, and Tectonics of the Serpentinites of the Zagros Suture Zone, Kurdistan Region, NE Iraq. Ph. D. Thesis. *University of Sulaimani*, p. 250

Azizi, H., Hadi, A., Asahara, Y., & Mohammad, Y. 2013. Geochemistry and geodynamics of the Mawat mafic complex in the Zagros Suture zone, northeast Iraq. *Open Geosciences*, 5(4), p. 523–537.

Belousova E.A., Griffin W.L. & O'Reilly S.Y., 2006. Zircon crystal morphology, trace element signatures and Hf isotope composition as a tool for petrogenetic modeling: examples from Eastern Australian granitoids. *Journal of Petrology,* 47(2), p. 329–353.

Buday, T. and Jassim, S.Z. 1987. The Regional Geology of Iraq. Tectonism, Magmatism and Metamorphism. *Geological Survey of Iraq*, 2, 352 pp.

Bouvier, A., Vervoort, J.D. & Patchett, P.J., 2008. The Lu–Hf and Sm–Nd isotopic composition of CHUR: constraints from unequilibrated chondrites and implications for the bulk composition of terrestrial planets. *Earth and Planetary Science Letters*, 273(1), p. 48–57.

Cawood, P. A., Kröner, A., Collins, W. J., Kusky, T. M., Mooney, W. D., & Windley, B. F. 2009. Accretionary orogens through Earth history. *Geological Society, London, Special Publications*, 318(1), p. 1–36.

Condie, K. C. 1993. Chemical composition and evolution of the upper continental crust: contrasting results from surface samples and shales. *Chemical Geology*, 104(1–4), p. 1–37.

Cox, J., Searle, M., & Pedersen, R. 1999. The petrogenesis of leucogranitic dykes intruding the northern Semail ophiolite, United Arab Emirates: field relationships, geochemistry and Sr/Nd isotope systematics. *Contributions to Mineralogy and Petrology*, 137(3), p. 267–287.

Defant, M. J., & Drummond, M. S. 1990. Derivation of some modern arc magmas by melting of young subducted lithosphere. *Nature*, 347(6294), p. 662–665.

Dilek, Y., Robinson, P.T. (Eds.), 2003. Ophiolites in Earth History.*Geological Society of London*. *Special Publication*. 218. 720 p.

Dilek, Y., & Ahmed, Z. 2003. Proterozoic ophiolites of the Arabian Shield and their significance in Precambrian tectonics. *Geological Society, London, Special Publications*, 218(1), p. 685–700.

Dilek, Y., Furnes, H., & Shallo, M. 2007. Suprasubduction zone ophiolite formation along the periphery of Mesozoic Gondwana. *Gondwana Research*, 11(4), p. 453–475.

Dilek, Y., & Furnes, H. 2009. Structure and geochemistry of Tethyan ophiolites and their petrogenesis in subduction rollback systems. *Lithos*, 113(1-2), p. 1–20.

Dilek, Y., Imamverdiyev, N., & Altunkaynak, Ş. 2010. Geochemistry and tectonics of Cenozoic volcanism in the Lesser Caucasus (Azerbaijan) and the peri-Arabian region: collision-induced mantle dynamics and its magmatic fingerprint. *International Geology Review*, 52(4-6), p. 536–578.

Dilek, Y., & Furnes, H. 2011. Ophiolite genesis and global tectonics: Geochemical and tectonic fingerprinting of ancient oceanic lithosphere. *Geological Society of America, Bulletin*, 123(3–4), p. 387–411.

Dilek, Y., & Furnes, H. 2014. Ophiolites and their origins. *Elements*, 10 (2), p. 93–100.

Fergusson, C. L., Nutman, A. P., Mohajjel, M., & Bennett, V. C. 2016. The Sanandaj–Sirjan Zone in the Neo-Tethyan suture, western Iran: Zircon U–Pb evidence of late Palaeozoic rifting of northern Gondwana and mid-Jurassic orogenesis. *Gondwana Research*, 40, p. 43–57.

Furnes, H., & Dilek, Y. 2017. Geochemical characterization and petrogenesis of intermediate to silicic rocks in ophiolites: A global synthesis. *Earth-Science Reviews*, 166, p. 1–37.

Furnes, H., Dilek, Y., Zhao, G., Safonova, I., & Santosh, M. 2020. Geochemical characterization of ophiolites in the Alpine-Himalayan Orogenic Belt: Magmatically and tectonically diverse evolution of the Mesozoic Neotethyan oceanic crust. *Earth-Science Reviews*, 208, 103258.

Gerdes A. & Zeh A., 2006. Combined U-Pb and Hf isotope LA-(MC-) ICPMS analyses of detrital zircons: Comparison with SHRIMP and new constraints for the provenance and age of an Armorican metasediment in Central Germany. *Earth and Planetary Science Letters*, 249(1-2), p. 47–61

Ghazi, J. M., Moazzen, M., Rahgoshay, M., & Moghadam, H. S. 2012. Geochemical characteristics of basaltic rocks from the Nain ophiolite (Central Iran); constraints on mantle wedge source evolution in an oceanic back arc basin and a geodynamical model. *Tectonophysics*, 574, p. 92–104.

Griffin, W. L., Pearson, N. J., Belousova, E., Jackson, S. V., Van Achterbergh, E., O'Reilly, S. Y., & Shee, S. R. 2000. The Hf isotope composition of cratonic mantle: LAM-MC-ICPMS analysis of zircon megacrysts in kimberlites. *Geochimica et Cosmochimica Acta*, *64*(1), p. 133–147.

Haase, K. M., Freund, S., Koepke, J., Hauff, F., & Erdmann, M. 2015. Melts of sediments in the mantle wedge of the Oman ophiolite. *Geology*, 43(4), p. 275–278.

Heinonen, A. P., Andersen, T. & Rämö, O. T., 2010. Re-evaluation of rapakivi petrogenesis: Source constraints from the Hf isotope composition of zircon in the rapakivi granites and associated mafic rocks of southern Finland. *Journal of Petrology*, 51(8), p. 1687–1709.

Hirano, N., Ogawa, Y., Saito, K., Yoshida, T., Sato, H., & Taniguchi, H. 2003. Multi-stage evolution of the Tertiary Mineoka ophiolite, Japan: new geochemical and age constraints. *Geological Society, London, Special Publications*, 218(1), p. 279–298.

Homke, S., Vergés, J., Van Der Beek, P., Fernàndez, M., Saura, E., Barbero, L., Badics, B., & Labrin, E. 2010. Insights in the exhumation history of the NW Zagros from bedrock and detrital apatite fission-track analysis: evidence for a long-lived orogeny. *Basin Research*, 22(5), p. 659–680.

Huhma, H., Mänttäri, I., Peltonen, P., Kontinen, A., Halkoaho, T., Hanski, E., Hokkanen, T., Hölttä, P., Juopperi, H., Konnunaho, J., Layahe, Y., Luukkonen. E., Pietikäinen. K., Pulkkinen, A., Sorjonen-Ward, P., Vaasjoki, M. & Whitehouse, M., 2012. The age of the Archaean greenstone belts in Finland. *Geological Survey of Finland, Special Paper*, 54, p. 74−175.

Ishizuka, O., Tani, K., & Reagan, M. K. 2014. Izu-Bonin-Mariana forearc crust as a modern ophiolite analogue. *Elements*, *10*(2), p. 115–120.

Ishikawa, A., Kaneko, Y., Kadarusman, A., & Ota, T. 2007. Multiple generations of forearc mafic–ultramafic rocks in the Timor–Tanimbar ophiolite, eastern Indonesia. *Gondwana Research*, 11(1–2), p. 200–217.

Ismail, S., & Al-Chalabi, S. 2006. Genesis of Chromitite in Qalander Area, Northern Iraq. *Kirkuk University Journal-Scientific Studies*, 1(2), p. 10–29.

Ismail, S. A., Arai, S., Ahmed, A. H., & Shimizu, Y. 2009. Chromitite and peridotite from Rayat, northeastern Iraq, as fragments of a Tethyan ophiolite. *Island Arc*, 18(1), p. 175–183.

Ismail, S. A., Mirza, T. M., & Carr, P. F. 2010. Platinum-group elements geochemistry in podiform chromitites and associated peridotites of the Mawat ophiolite, northeastern Iraq. *Journal of Asian Earth Sciences*, 37(1), p. 31–41.

Ismail, S. A., Kettanah, Y. A., Chalabi, S. N., Ahmed, A. H., & Arai, S. 2014. Petrogenesis and PGE distribution in the Al-and Cr-rich chromitites of the Qalander ophiolite, northeastern Iraq: Implications for the tectonic environment of the Iraqi Zagros Suture Zone. *Lithos*, 202, p. 21–36.

Ismail, S. A., Ali, S. A., Nutman, A. P., Bennett, V. C., & Jones, B. G. 2017. The Pushtashan juvenile suprasubduction zone assemblage of Kurdistan (northeastern Iraq): A Cretaceous (Cenomanian) Neo-Tethys missing link. *Geoscience Frontiers*, 8(5), p. 1073–1087.

Ismail, S. A., Koshnaw, R. I., Barber, D. E., Al Humadi, H., & Stockli, D. F. 2020. Generation and exhumation of granitoid intrusions in the Penjween ophiolite complex, NW Zagros of the Kurdistan region of Iraq: Implications for the geodynamic evolution of the Arabian-Eurasian collision zone. *Lithos*, 376, 105714.

Jahn, B. M. 1986 Mid-ocean ridge or marginal basin origin of the East Taiwan Ophiolite: chemical and isotopic evidence. *Contribution to Mineralogy and Petrology*, 92(2), p. 194–206.

Janoušek, V., Farrow, C. M., & Erban, V. 2006. Interpretation of whole-rock geochemical data in igneous geochemistry: introducing Geochemical Data Toolkit (GCDkit). *Journal of Petrology*, 47(6), 1255–1259.

Jassim, S. Z. 1973. Geology of the central sector of Mawat complex. *Journal of Geological Society of Iraq*, 6. p. 82–92

Jassim, S. Z., & Goff, J. C. (Eds.). 2006. Geology of Iraq. Dolin, Prague and Moravian Museum, Brno, 341 p.

Kontinen, A. 1987. An early Proterozoic ophiolite—the Jormua mafic-ultramafic complex, northeastern Finland. *Precambrian Research*, 35, 313–341.

Koshnaw R.I., Stockli D.F. and Schlunegger F., 2018, Timing ofthe Arabia-Eurasia continental collision Evidence from detritalzircon U-Pb geochronology of the Red Bed Series strata of thenorthwest Zagros hinterland, Kurdistan region of Iraq. *Geology*, 47, p. 47–50.

Koyi, A. M. A., Sofyissa, M. M., & Jameel, N. M. 2010. Geochemistry of Metagabbros from Southern Mawat Ophiolite Complex, NE Iraq. Journal of Pure Sciences, Salahddin University, V 22 No. 4.

Kusky, T.M. (Ed.), 2004. Precambian Ophiolites and Related Rocks. Developments in Precabrian Geology, 13, *Elsevier, Amsterdam*. 748 p.

Kusky, T. M., Wang, L., Dilek, Y., Robinson, P., Peng, S., & Huang, X. 2011. Application of the modern ophiolite concept with special reference to Precambrian ophiolites. *Science China Earth Sciences*, 54(3), p. 315–341.

Lippard, S. J., Shelton, A. W., & Gass, I. G. 1986. The Ophiolite of Northern Oman. *Geological Society of London*, Memoir 11 178 p.

Ludwig, K. R. 2003. User's Manual for Isoplot/ex, 3.00. A geochronological toolkit for Microsoft excel. *Berkeley Geochronology Center Special Publication,* 4, p. 25–32.

Martin, H. 1999. Adakitic magmas: modern analogues of Archaean granitoids. *Lithos*, *46*(3), p. 411–429.

Mirza, T. A., & Ismail, S. A. 2007. Origin of plagiogranite in the Mawat ophiolite complex, Kurdistan Region, NE Iraq. *Journal of Kirkuk University–Scientific Studies*, *2*, p. 1–25.

Moghadam, H. S., & Stern, R. J. 2011. Late Cretaceous forearc ophiolites of Iran. *Island Arc*, 20(1), p. 1–4.

Moghadam, H. S., & Stern, R. J. (2014). Ophiolites of Iran: Keys to understanding the tectonic evolution of SW Asia: (I) Paleozoic ophiolites. *Journal of Asian Earth Sciences*, *91*, p. 19–38.

Moghadam, H. S., Corfu, F., Chiaradia, M., Stern, R. J., & Ghorbani, G. 2014. Sabzevar Ophiolite, NE Iran: Progress from embryonic oceanic lithosphere into magmatic arc constrained by new isotopic and geochemical data. *Lithos*, 210, p. 224–241.

Moghadam, H. S., Corfu, F., Stern, R. J., & Bakhsh, A. L. 2019. The Eastern Khoy metamorphic complex of NW Iran: a Jurassic ophiolite or continuation of the Sanandaj–Sirjan Zone? *Journal of the Geological Society*, 176(3), p. 517–529.

Mohajjel, M., & Fergusson, C. L. 2014. Jurassic to Cenozoic tectonics of the Zagros Orogen in northwestern Iran. *International Geology Review*, 56(3), p. 263–287.

Mohammad, Y. O., Cornell, D. H., Qaradaghi, J. H., & Mohammad, F. O. 2014. Geochemistry and Ar–Ar muscovite ages of the Daraban Leucogranite, Mawat Ophiolite, northeastern Iraq: implications for Arabia–Eurasia continental collision. *Journal of Asian Earth Sciences*, 86, p. 151–165.

Mohammad, Y. O., & Qaradaghi, J. H. 2016. Geochronological and mineral chemical constraints on the age and formation conditions of the leucogranite in the Mawat ophiolite, Northeastern of Iraq: insight to sync-subduction zone granite. *Arabian Journal of Geosciences*, 9(12), p. 1–23.

Mohammad, Y. O., & Cornell, D. H. 2017. U–Pb zircon geochronology of the Daraban leucogranite, Mawat ophiolite, Northeastern Iraq: a record of the subduction to collision history for the Arabia–Eurasia plates. *Island Arc*, 26(3), p. 1–12.

Moores, E. M. 1982. Origin and emplacement of ophiolites. *Reviews of Geophysics*, 20(4), p. 735–760.

Morel, M. L. A., Nebel O., Nebel-Jacobsen Y. J., Miller J. S. & Vroon P. Z., 2008. Hafnium isotope characterization of the GJ-1 zircon reference material by solution and laser-ablation MC-ICPMS. *Chemical Geology*, 255(1-2), P. 231–235.

Moyen, J. F. 2009. High Sr/Y and La/Yb ratios: the meaning of the "adakitic signature". *Lithos*, 112(3-4), p. 556–574.

Numan, N. M. 1997. A plate tectonic scenario for the Phanerozoic succession in Iraq. *Iraqi Geological Journal*, 30(2), p. 85–110.

Parson, L. M., Murton, B. J., Browning, P., 1992. Ophiolites and Their Modern Oceanic Analogues. *Geological Society, Special Publication*, 60: 330 p.

Pearce, J. A. 2008. Geochemical fingerprinting of oceanic basalts with applications to ophiolite classification and the search for Archean oceanic crust. *Lithos*, 100(1–4), 14–48.

Pedersen, R. B., & Malpas, J. 1984. The origin of oceanic plagiogranites from the Karmoy ophiolite, western Norway. *Contributions to Mineralogy and Petrology*, 88(1–2), p. 36–52.

Reagan, M. K., Ishizuka, O., Stern, R. J., Kelley, K. A., Ohara, Y., Blichert-Toft, J., Bloomer, S.H., Cash, J., Fryer, P., Hanan, B.B., Hickey-Vargas, R., Ishii, T., Kimura-I, J., Peate, D. W., Rowe, M.C. & Woods, M. 2010. Fore-arc basalts and subduction initiation in the Izu-Bonin-Mariana system. *Geochemistry, Geophysics, Geosystems*, *11*(3). p. 1–17. 2009GC002871

Robertson, A. H., Parlak, O., & Ustaömer, T. 2013. Late Palaeozoic–Early Cenozoic tectonic development of Southern Turkey and the easternmost Mediterranean region: evidence from the inter-relations of continental and oceanic units. *Geological Society, London, Special Publications*, 372(1), p. 9–48.

Rollinson H.R., 1993. Using geochemistry data: Evaluation, presentation, interpretation. *Longman Sci. Techn. Ltd., Essex*, 352 pp.

Rollinson, H. 2014. Plagiogranites from the mantle section of the Oman Ophiolite: models for early crustal evolution. *Geological Society, London, Special Publications*, 392(1), p. 247–261.

Rollinson, H. 2015. Slab and sediment melting during subduction initiation: granitoid dykes from the mantle section of the Oman ophiolite. *Contributions to Mineralogy and Petrology*, 170(3), p. 1–20.

Rosa D. R. N., Finch A. A., Andersen T. & Inverno C. M. C., 2009. U-Pb geochronology and Hf isotope ratios of magmatic zircons from the Iberian pyrite belt. *Mineralogy and Petrology*, 95(1–2), p. 47–69.

Saccani, E., Padoa, E., & Photiades, A. 2003. Triassic mid-ocean ridge basalts from the Argolis Peninsula (Greece): new constraints for the early oceanization phases of the Neo-Tethyan Pindos basin. *Geological Society, London, Special Publications*, 218(1), p. 109–127.

Santosh, M., Teng, X. M., He, X. F., Tang, L., & Yang, Q. Y. 2016. Discovery of Neoarchean suprasubduction zone ophiolite suite from Yishui Complex in the North China Craton. *Gondwana Research*, 38, p. 1–27.

Shervais, J. W., Reagan, M., Haugen, E., Almeev, R. R., Pearce, J. A., Prytulak, J., Ryan, J. G., Whattam,S. A., Godard, M., Chapman, T., Li, H., Kurz, W., Nelson, W. R., Heaton, D., Kirchenbaur, M., Shimizu, K., Sakuyama, T., Li, Y., & Vetter, S. K. 2019. Magmatic response to subduction initiation: Part 1. Fore-arc basalts of the Izu-Bonin arc from IODP Expedition 352. *Geochemistry, Geophysics, Geosystems*, 20(1), p. 314–338.

Sláma, J., Košler, J., & Pedersen, R. B. 2007. Behaviour of zircon in high-grade metamorphic rocks: evidence from Hf isotopes, trace elements and textural studies. *Contributions to Mineralogy and Petrology*, 154(3), p. 335–356.

Veloso, E. A. E., Anma, R., & Yamazaki, T. 2005. Tectonic rotations during the Chile Ridge collision and obduction of the Taitao ophiolite (southern Chile). *Island Arc*, 14(4), p. 599–615.

Verdel, C., Wernicke, B. P., Hassanzadeh, J., & Guest, B. 2011. A Paleogene extensional arc flare-up in Iran. *Tectonics*, *30*(3), p. 1–20

Yumul Jr, G. P. 2007. Westward younging disposition of Philippine ophiolites and its implication for arc evolution. *Island Arc*, 16(2), p. 306–317.

Zhang, Z., Xiao, W., Ji, W., Majidifard, M. R., Rezaeian, M., Talebian, M., Xiang, D., Chen, L., Wan, B., Ao, S., & Esmaeili, R. 2018. Geochemistry, zircon U-Pb and Hf isotope for granitoids, NW Sanandaj-Sirjan zone, Iran: Implications for Mesozoic-Cenozoic episodic magmatism during Neo-Tethyan lithospheric subduction. *Gondwana Research*, *62*, p. 227–245.

TURUN
YLIOPISTO
UNIVERSITY
OF TURKU

Painosalama, Turku, Finland 2021

ISBN 978-951-29-8658-3 (PRINT)
ISBN 978-951-29-8659-0 (PDF)
ISSN 0082-6979 (Print)
ISSN 2343-3183 (Online)